Running speed changes the distribution of excitation within the biceps femoris muscle in 80m sprints

Received: 2 November 2022 | Revised: 12 February 2023 | Accepted: 16 February 2023

DOI: 10.1111/sms.14341

ORIGINAL ARTICLE

WILEY

Running speed changes the distribution of excitation within the biceps femoris muscle in 80 m sprints

Giacinto L. Cerone[1,2] | **Riccardo Nicola**[1] | **Marco Caruso**[2] | **Rachele Rossanigo**[3] | **Andrea Cereatti**[2] | **Taian Martins Vieira**[1,2]

[1]Laboratory for Engineering of the Neuromuscular System, Department of Electronics and Telecommunications, Politecnico di Torino, Turin, Italy

[2]Polito[BIO]Med Lab—Biomedical Engineering Lab and Department of Electronics and Telecommunications, Politecnico di Torino, Torino, Italy

[3]Department of Biomedical Sciences, University of Sassari, Sassari, Italy

Correspondence
Taian Martins Vieira, Laboratory for Engineering of the Neuromuscular System, Department of Electronics and Telecommunications, Politecnico di Torino, Corso Duca degli Abruzzi 24, Turin 10129, Italy
Email: taian.martins@polito.it

Predictors and mitigators of strain injuries have been studied in sprint-related sports. While the rate of axial strain, and thus running speed, may determine the site of muscle failure, muscle excitation seemingly offers protection against failure. It seems therefore plausible to ask whether running at different speeds changes the distribution of excitation within muscles. Technical limitations undermine, however, the possibility of addressing this issue in high-speed, ecological conditions. Here, we circumvent these limitations with a miniaturized, wireless, multi-channel amplifier, suited for collecting spatio-temporal data and high-density surface electromyograms (EMGs) during overground running. We segmented running cycles while 8 experienced sprinters ran at speeds close to (70% and 85%) and at (100%) their maximum, over an 80 m running track. Then, we assessed the effect of running speed on the distribution of excitation within biceps femoris (BF) and gastrocnemius medialis (GM). Statistical parametric mapping (SPM) revealed a significant effect of running speed on the amplitude of EMGs for both muscles, during late swing and early stance. Paired SPM revealed greater EMG amplitude when comparing 100% with 70% running speed for BF and GM. Regional differences in excitation were observed only for BF, however. As running speed increased from 70% to 100% of the maximum, a greater degree of excitation was observed at more proximal BF regions (from 2% to 10% of the thigh length) during late swing. We discuss how these results, in the context of the literature, support the protective role of pre-excitation against muscle failure, suggesting the site of BF muscle failure may depend on running speed.

KEYWORDS
hamstrings, high-density surface EMG, overground running, statistical parametric mapping

1 | INTRODUCTION

Athletes engaged in sprint-related sports often experience strain injuries of the lower limb muscles.[1–3] In athletics, for instance, muscle injuries were reported to have affected nearly 35% of athletes participating in international championships, with the sprint discipline being the main culprit.[4,5] During sprints, injuries appear to manifest more often in the hamstring muscles, followed by the posterior leg.[4] Conceivably, given the displeasing,

frustrating consequences of muscle injury, a myriad of studies emerged and contributed to the identification of factors helping to predict and mitigate muscle injury during sprints. Two, cogent information has been disclosed. First, animal preparations revealed the maximal degree of strain to be the determinant of muscle failure,[6,7] supporting the notion that hamstring injuries take place when the muscle reaches maximal elongation during the running cycle—late swing and late stance.[8,9] Second, animal models further revealed that, before tearing, muscles have a much greater potential to store energy when being pulled while contracted than while at rest.[10] Considering the degree of hamstring excitation is greater when it is maximally elongated during the running cycle,[11,12] it has been therefore suggested that excitation could help protecting the muscle against tearing.[13] Notwithstanding these insights, a still unexplored issue is whether muscle excitation, and thus the potential to prevent failure, is site dependent or not during running.

The possibility that failure may occur at different muscle locations stems from observations that the site of failure depends on the rate of muscle strain. When increasing the rate of axial strain from 40 cm/s to 100 cm/s in tissue preparations, Best et al.[6] observed the maximal strain, and thus the site of failure, to occur, respectively, at the muscle-tendon junction and at the muscle belly. Given the putative view that muscle excitation protects from tearing, it is therefore likely that regional differences in muscle excitation may be observed for different loading rates and thus running speeds. Pieces of evidence have documented the effect of running speed on the degree of excitation of different lower limb muscles, revealing greater speeds to generally impose greater, excitation demands.[11,14,15] In these studies, muscle excitation has been inferred from the amplitude of surface electromyograms (EMGs) detected from a single, muscle location, precluding the possibility of assessing site-specific changes in excitation with running speed. Recently, however, Hegyi et al.[13] used an array of electrodes to sample surface EMGs from different sites in biceps femoris (BF) and semitendinous, revealing no effect of running speed on the distribution of excitation across the proximo-distal region of both muscles. In spite of their rigorous, methodological approach, based on high-density surface EMG (HD-EMGs[16]), the study of Hegyi et al.[13] was limited to treadmill running and to submaximal (up to 75%) running speeds. The encumbrance offered by conventional systems for HD-EMG acquisition is presumably the limiting factor for assessing regional changes in muscle excitation in more ecological conditions. Considering, however, the metabolic and kinematic differences between treadmill and overground running, with the former being associated with lower degrees of excitation of lower limb muscles,[17] reduced and increased range of motion in swing and stance phases, respectively,[18,19] and less energy expenditure for a given running speed,[19] the relevance of extending the pioneering work of Hegyi et al.[13] to overground sprints appears justified.

In this study, we investigate this issue with miniaturized, wearable systems developed in our laboratory for the acquisition of HD-EMG[20] and of running spatio-temporal data.[21] Both systems can be synchronized between themselves and with third party devices, opening for the conception of protocols not limited to laboratory settings. Here, indeed, we use both systems to assess whether, within the running cycle, the distribution of muscle excitation in high-performance athletes depends on running speed during overground running. We specifically ask whether the distribution of EMG amplitude in BF and gastrocnemius medialis (GM) changes when sprint athletes run at velocities progressively closer to their maximal speed. The range of running speeds covered here, from 70% to 100% of maximal sprint speed, complements that assessed previously with HD-EMG during treadmill running.[13] We expect the amplitude of EMGs to increase with running speed.[11,14,15] Most importantly, if increasing running speed changes the site of maximal strain, as reported for greater loading rates in animal preparations,[6] we further expect to observe regional changes in the distribution of EMG amplitude with running speed (i.e., a shift in peak excitation towards the muscle belly). In addition to advancing our knowledge on the spatial pattern of excitation of two powerful, extensor muscles, often injured muscles during high-speed running,[4,22] our results likely posit a methodological reference for the assessment of muscle excitation with surface EMG during overground running.

2 | METHODS

2.1 | Subjects

Ten male athletes (range: 19–31 years; 59–83 kg; 1.68–1.98 m) volunteered to participate in the study, after being informed on the experimental procedures and providing written, informed consent. All subjects were experienced runners, training over five times a week, being engaged in competitive events for at least 3 years, and scoring over 700 points in the tables of World Athletics in one of the velocity disciplines[23]—that is, taking less than 11.66 s to cover the 100 m distance. None of the participants reported to have had any musculoskeletal injury or any complication hindering their sprinting ability within the preceding 6 months. The experimental procedures conformed to the Declaration of Helsinki and were approved by the Regional Ethics Committee.

2.2 | Experimental protocol

Subjects were first asked to warm-up freely for roughly 40 min. They were allowed to run at self-selected speeds as they found fit, from slow jogging to running at submaximal speed using the same track spikes they use during competitions—athletes used their own, preferred spikes. The warm-up session was sought to suppress any potential muscle damage arising during the experimental trials, wherein subjects were requested to run at maximal speed.[24] After warm-up, subjects performed an 80 m sprint straight over one lane of an official, 400 m track. The sprint started with the subject in the crouch three-point position (Figure 1A), upon the issuing of an audio command from the experimenter. The duration of the sprint trial was measured with a hand chronometer (Motus chronometry millennium MT50, sensitivity 1 ms) and then taken as a reference to define the maximal, average running speed. Similar to the study of Kuitunen et al.[15] once the sprint trial was completed and over the same 80 m piece of the running track, subjects were asked to run twice at three different speeds: 70%, 85%, and 100% of the maximal speed. The six trials (two repetitions × three speeds) were applied in random order, with at least 5 min of recovery in-between to prevent fatigue buildup and while wearing the acquisition systems described below (Figure 1A). No feedback other than the time taken to cover the 80 m distance during the sprint trial was provided and all athletes declared to be able to run at the requested, average speed.

2.3 | Muscle excitation and contact events

Monopolar surface EMGs were detected from GM and BF with two, high-density systems of electrodes, after cleaning the skin with abrasive paste (Nuprep® Skin Prep Gel, Weaver and Company). For the GM muscle, EMGs were sampled with a linear array of 32 surface electrodes (5 mm inter-electrode distance; IED). The array was aligned parallel to the muscle longitudinal axis, positioned at the bulk of the muscle and with the most proximal electrode located 2 cm distally to the popliteal fossa.[25] For BF, an anisotropic matrix of 32 surface electrodes was used (16 rows and 2 columns, 15 mm IED between rows and 10 mm between columns). The matrix was centered at the location where bipolar EMGs have been recommended to be detected from BF.[26] Columns were aligned along the muscle longitudinal direction, identified visually. For all participants, the BF muscle was clearly visible from the skin when

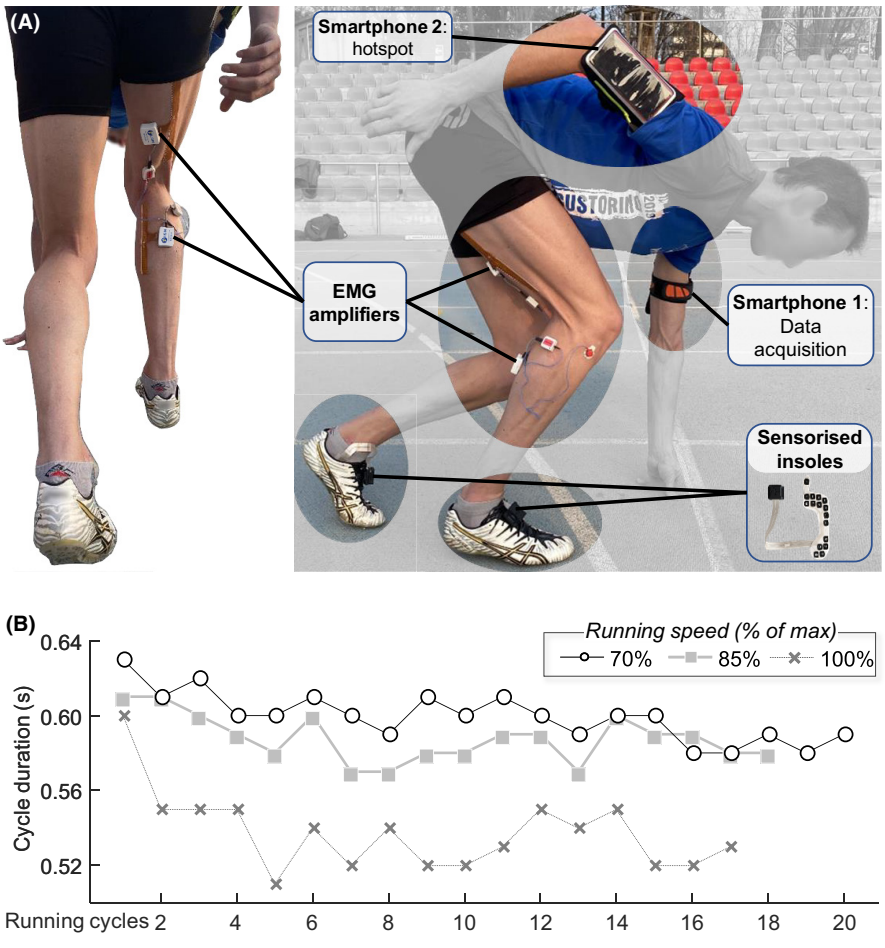

FIGURE 1 Subject setup and duration of running cycles. (A) The two Wi-Fi modules for the sampling of high-density surface EMGs (HD-EMGs) and the two sensorized insoles for running cycle identification are shown. The thin cables connecting the reference electrode to the Wi-Fi modules were tightened with an elasticized bandage (Previcoesiva LF, Vicenza, Italy) to minimize movement artifacts. (B) duration of each running cycle for each of the three running speeds (○: 70%; ■: 85%; ×: 100% of maximal running speed) is shown for a representative participant.

gently flexing the knee against manual resistance. For the two muscles, arrays were secured to the skin with adhesive pads, with holes being punched in correspondence of the location of electrodes and filled with conductive paste (Ten20® conductive paste, Weaver and Company).

High-density surface EMGs were recorded using a modular, wireless system.[20] After amplification (192 V/V), EMGs were sampled at 2048 Hz with a 16-bit A/D converter. Two smartphones were used for the collection of EMGs (Figure 1A). One smartphone (Samsung Galaxy S20), the server, was used to communicate with clients—two EMG acquisition modules, each connected to one electrode array. The other smartphone (Redmi Note 9 Pro) was used as a router, establishing the network through which clients and server could communicate. Smartphones were secured to the left and right arms with elastic bands, minimizing any running hindrance. With this setup, no data were lost because clients and server were kept in proximity throughout the 80 m, running trials.

Running-related events were assessed using the INertial module with DIstance Sensors and Pressure insoles,[21] including two three-axial inertial measurement units, each connected to one, extra-thin pressure insole.[21] The insole encloses a set of 16 pressure sensors (mod. YETI, 221 e S.r.l., Padua, Italy; element area = 310 mm^2; ground reaction force threshold = 5 N), distributed between the fore and hindfoot. During experimental trials all subjects were requested to wear their preferred shoes, into which the insoles were inserted. Pressure and inertial data were sampled at 100 Hz and stored into a datalogger housed within the insole controlling unit (Figure 1A). The offline synchronization of the 64 EMGs and the data from the instrumented insoles was ensured through a common trigger pulse (500 ms, 0–5 V TTL),[27] issued concomitantly to both systems via radiofrequency (EMG) and Bluetooth (insoles) protocols.

2.4 | Data analysis

Pressure insoles involved in the experimental setup were previously validated for the identification of gait events.[28] In this study, the foot-mounted system was used to segment the running cycles, defined by two consecutive initial contacts with the ground for the same foot. First of all, a quality check on the pressure insoles data was performed to exclude potential low-quality pressure sensors data. Then, sharp rising edges in correspondence of the instants of impact with the ground were identified from the first derivative of the pressure signals.[28] The initial contact search window was defined for at least two pressure sensors, both providing the beginning of the rising edge within less than 0.1 s of discrepancy. The initial contact instant was then identified as the last rising edge within the search window.

Monopolar EMGs were first visually inspected, and low-quality signals (cf.[16]) were linearly interpolated with their neighbors. Single-differential EMGs were computed for consecutive, monopolar signals, after band-pass filtering each monopolar signal with a zero-lag, Butterworth filter (fourth order, 20–400 Hz cutoff; Figure 2). Differential EMGs were computed in the longitudinal and transverse directions for GM and BF, respectively, maximizing the representation of proximo-distal excitation for both muscles. That is, we would have lost 15 mm of BF proximo-distal coverage had we computed differential EMGs longitudinally along the array. After that, the differential EMGs were full-wave rectified and low-pass filtered (second order, Butterworth filter, 10 Hz cutoff[13]), producing a set of EMG envelopes per muscle. For the GM muscle, channels located over skin regions parallel to the muscle fibers were excluded from analysis, ensuring like-with-like comparisons proximo-distally across the muscle (Figure 3; cf. figure 6 in[16]). For the BF muscle, because of inter-individual differences in thigh length, not all rows of electrodes covered the muscle. In such cases ($n = 6$; Figure S1), being the array longer than the muscle, only EMGs detected by rows of electrodes located over the muscle were considered for analysis. For both muscles, EMG envelopes were then segmented into individual running cycles based on data from the INDIP system. The mean EMG value over epochs corresponding to 2% of the running cycle was computed and averaged across channels and cycles,[29] after discarding cycles within the first 30% of each running trial (Figure 1B). Initial cycles were discarded to contend with the effect of the acceleration phase on muscle excitation and, thus, on the distribution of EMG amplitude. This procedure provided 50 amplitude values per EMG considered, separately for each muscle and for each of the three running speeds tested (Figure 4A). Regional differences in muscle excitation with running speed were assessed through the centroid of channels providing EMG envelopes higher than 70% of the maximum.[30] The segmented channels are expected to provide a coarse estimation of the size of the excited muscle region whereas the centroid indicates where the excited region is centered in the muscle (cf. figure 4 in[16])—centroids were computed only for temporal clusters of EMG envelopes statistically dependent on running speed and then normalized with respect to the leg (GM) and thigh (BF) lengths.

2.5 | Statistics

Statistical parametric mapping (SPM)[31] was applied to test for whether EMG envelopes changed with speed during the running cycle. This procedure has proved to be more robust

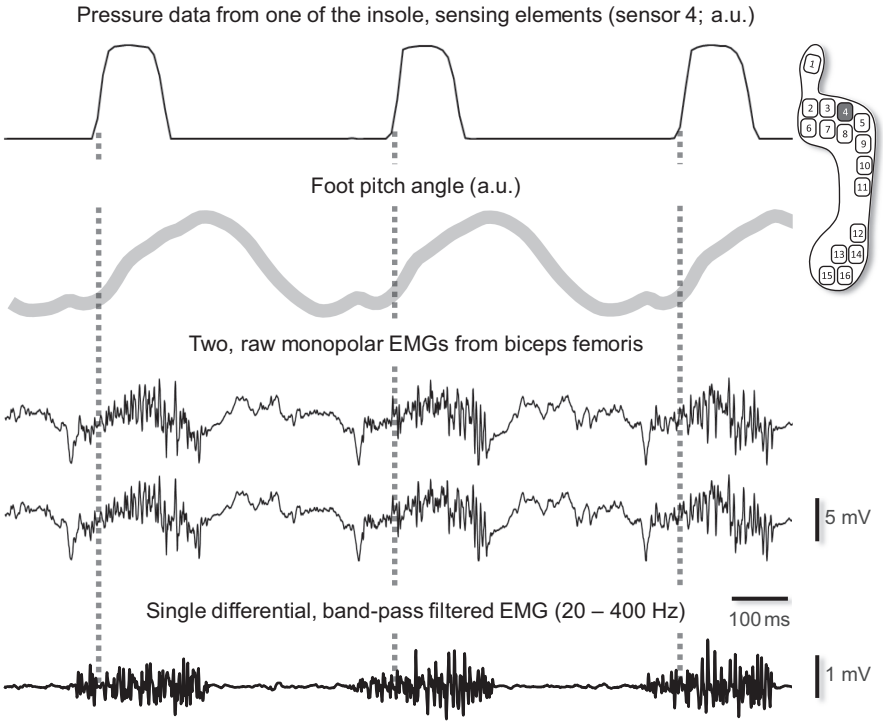

FIGURE 2 Segmentation of running cycles and computation of differential EMGs. Foot contact was determined based on the pressure data from the right foot insole, defining individual strides and thus running cycles. Slow, baseline fluctuations were evident in monopolar EMGs, with a temporal profile similar to the magnetic data associated with foot movement in the parasagittal plane. These common mode, slow fluctuations were suppressed after computing and band-pass filtering the single-differential EMGs.

to both Type I and Type II errors than the conventional, univariate approach applied to a scalar value computed from time series of biomechanical and electrophysiological data.[32] Briefly, we computed the univariate F statistic considering the 50 normalized time points—the 50 consecutive percentiles of the running cycle—and a design matrix with 12 columns of dummy variables,[33] corresponding to running speed ($n = 3$) and subject ($n = 8$) effects. This procedure resulted in a scalar field of F values, denoted as SPM{F}, for assessing within subjects effect. The main issue here is the determination of the critical test statistics associated with the imposed ($\alpha = 0.05$) statistical significance. For example, the family wise error would inflate should the critical F be determined arbitrarily for any of the 50 time points.[32] Similarly, correction of the significance level (e.g., Bonferroni correction) would be overconservative as the 50 time points are unlikely independent.[32,34] Random field theory was therefore applied to compute the critical test statistic more accurately associated with the 5% significance level. This procedure considers the smoothness of time series when defining the critical, test statistics—that is, how high and how temporally broad EMG descriptors are clustered within the running cycle. The p value associated with each cluster indicates the probability that a cluster similarly high (EMG envelope value) and broad (across the running cycle) would be attributable to an equally smooth, random fluctuation.

Whenever SPM{F} revealed an effect of running speed, SPM{t} was applied for post hoc assessment with Bonferroni correction. The field of t statistics for each paired analysis was computed as $t_i = \mathbf{c}.\mathbf{b}_i / \epsilon_i$, where $\mathbf{b}_i = \left[\beta_i^{70\%} \;\; \beta_i^{85\%} \;\; \beta_i^{100\%}\right]^T$ corresponds to the least square estimates of regressors associated with running at 70%, 85%, and 100% of maximal speed for the i-th time point. $\mathbf{c}$ is the contrast vector, determining the paired comparison of interest (e.g., $\mathbf{c} = \begin{bmatrix} -1 & 1 & 0 \end{bmatrix}$ for testing the hypothesis that $\beta_i^{70\%} < \beta_i^{85\%}$) and ϵ is the standard error associated with the hypothesis test determined by the contrasts. Similar to SPM{F}, random field theory was applied to compute the critical t value.

Whenever a cluster of SPM{t} values exceeding the critical threshold was identified, the EMG image within such period was processed for centroids. The effect of speed on the centroid location was assessed with the paired Student's t-test with Bonferroni correction.

3 | RESULTS

3.1 | Compliance with the experimental protocol

Subjects were able to run at speeds roughly close to the requested value. The median (1st-3rd quartiles) time

*Critical test statistics were also computed using permutations. Permutations and random field theory provided comparable (within 10%) test statistics, justifying the assumption of Gaussian distribution of residuals.[35] We nevertheless decided to proceed with the parametric approach for the critical test statistics because they were greater (by 5%) w.r.t. to those obtained with permutations, being therefore less prone to familywise error.

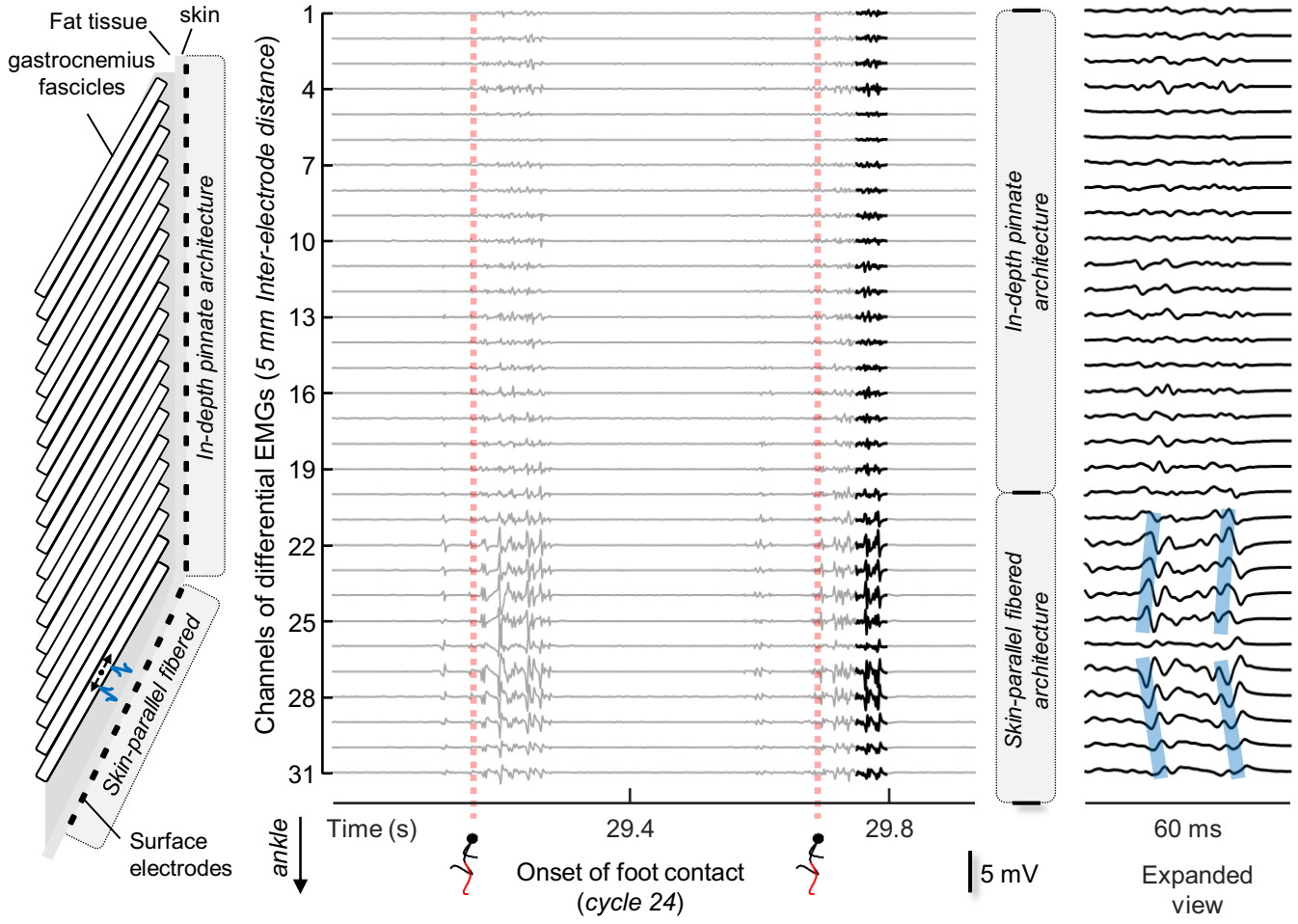

FIGURE 3 Identification of channels to include for analysis in the gastrocnemius muscle. Only channels located over the muscle superficial aponeurosis were retained, where gastrocnemius architecture is in-depth pennate from an EMG perspective.[16] These channels were identified as not providing the typical features—innervation zone and action potential propagation—observed when consecutive channels are aligned parallel to the muscle fibers. Both features may be observed only in the very distal extremity of the muscle, where fibers are disposed parallel to the skin.

taken to complete the 80 m track during the first sprint, while not wearing any acquisition system, was 9.207 (9.098–9.403 s). During the experimental trials at 70%, 85%, and 100% of the sprint speed, subjects, respectively, took 13.201 s (12.151–13.751 s), 11.091 s (10.681–11 510 s), and 9.255 s (9.210–9.405 s) to complete 80 m. When normalized to the sprint speed, the relative speed for the three consecutively greater speeds was 70.18% (68.12%–75.00%), 83.48% (79.66%–87.04%), and 98.91% (98.90%–98.95%).

3.2 | Effect of running speed on EMG amplitude

Because of technical issues, data from two subjects were discarded. For one subject, we realized to have not collected the trigger signal, because the cable from the trigger device was broken. For the other subject, the trigger signal was recorded for the EMG probes though not for the insoles.

Based on data from the remaining eight subjects, the SPM{*F*} revealed an effect of running speed on the EMG envelopes for the two muscles assessed. For GM, a large and high cluster of *F* values exceeding the critical threshold was observed at late swing and early stance whereas for BF a similarly large cluster was evident at late swing (Figure 4B). Other significant, even though short and small, clusters of over-threshold *F* values were observed for both muscles. Post hoc assessments revealed significant, paired differences only in correspondence of the large clusters of *F* values. During late stance, from roughly 75% to 100% of the cycle, large clusters of significant *t* values were observed for the two muscles, when comparing 70% versus 100% of the max running speed (Figure 4C). A small, though significant cluster of over-threshold *t* values was observed for BF between 85% and 100% of the maximal speed from 78% to 84% of the cycle.

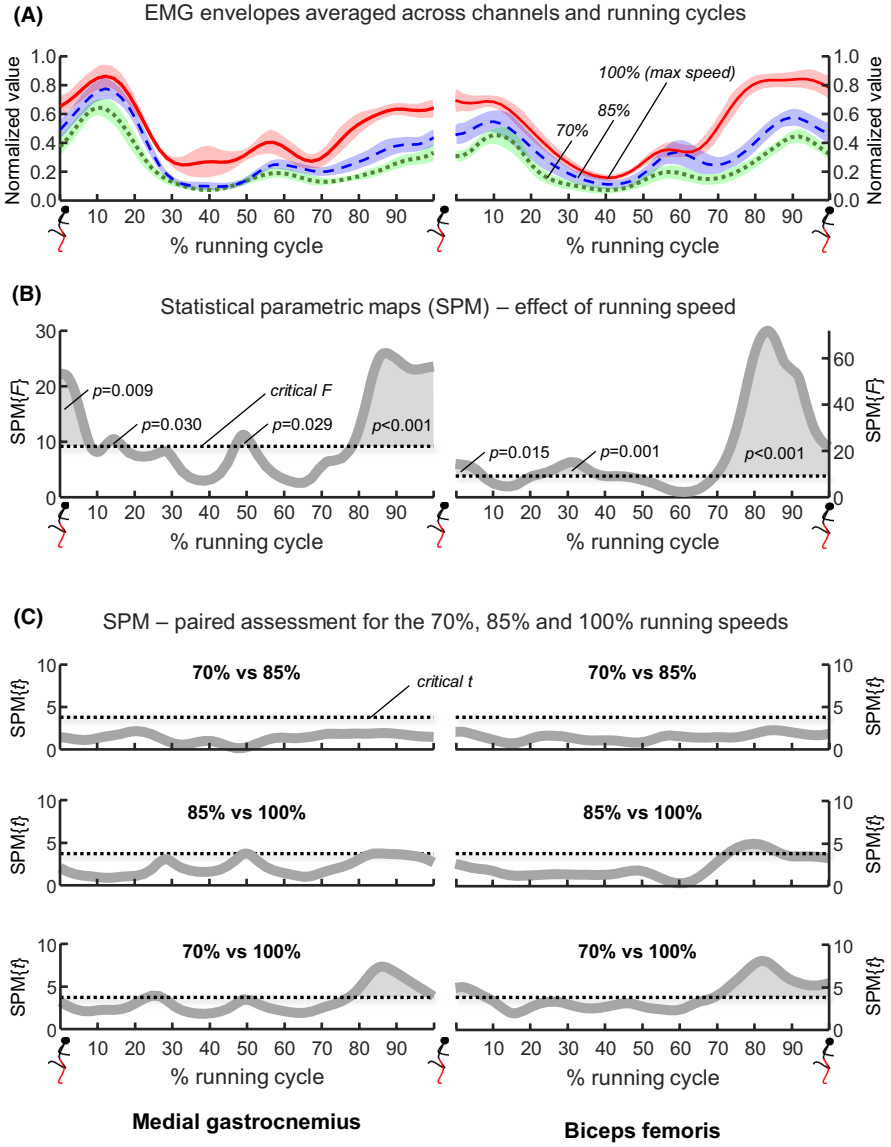

FIGURE 4 Group results for EMG envelopes. (A) EMG envelopes averaged across cycles and channels. For the sake of clarity, mean (thick traces) and standard error values are shown, with mean values being normalized with respect to the greatest amplitude value across cycles and channels. (B) statistical parametric map (SPM) created for the *F* statistics across the mean, running cycle. (C) SPM computed for the *t* statistics, summarizing each of the three paired assessments for the three running speeds tested, 70%, 80%, and 100% of the maximal speed. Dotted, horizontal lines denote the critical *F* (A) and *t* statistics (B), after Bonferroni correcting the later. Shaded clusters over the critical thresholds are unlikely due to chance at the *p* values reported for each.

3.3 | Effect of running speed on the distribution of EMG amplitude

The location within the BF muscle where greatest EMGs were detected differed between running speeds. When comparing 70% and 100% running speeds, during late swing, the centroid of EMG amplitude moved proximally by ~2 cm, for the single participant shown in Figure 5A, and by ~5% of the thigh length for the group data (Figure 5B; Student's paired *t*-test, $p = 0.032$ after Bonferroni correction). As shown in Figure 5B, for the other SPM{*t*} clusters reaching statistical significance (Figure 4C), running speed did not affect the location of centroids in the array ($p > 0.381$).

4 | DISCUSSION

In this study, we tested the hypothesis that overground running at different speeds would affect the amplitude distribution of surface EMGs. With arrays of electrodes, we sampled surface EMGs proximo-distally from BF and GM, while eight experienced athletes ran at 70%, 85%, and 100% of their maximal speed over a straight, 80 m track. Results revealed a significant effect of running speed on EMG amplitude. For the two muscles, running at 100% of the maximal speed resulted in significantly greater EMGs during late stance (Figure 4). Only for BF, greater EMG envelopes were detected more proximally in the muscle when running speed increased from 70% to 100% of maximal speed (Figure 5). Our results indicate both the degree and the proximo-distal location of BF excitation change with running speed at late swing, substantiating the need to explore site-specific associations between changes in BF architecture and excitation during running.

Before discussing our results, a note on the quality of EMGs recorded is warranted. There are multiple sources, other than the recruitment and rate coding of motor units, affecting the amplitude of EMGs. Muscle and cable

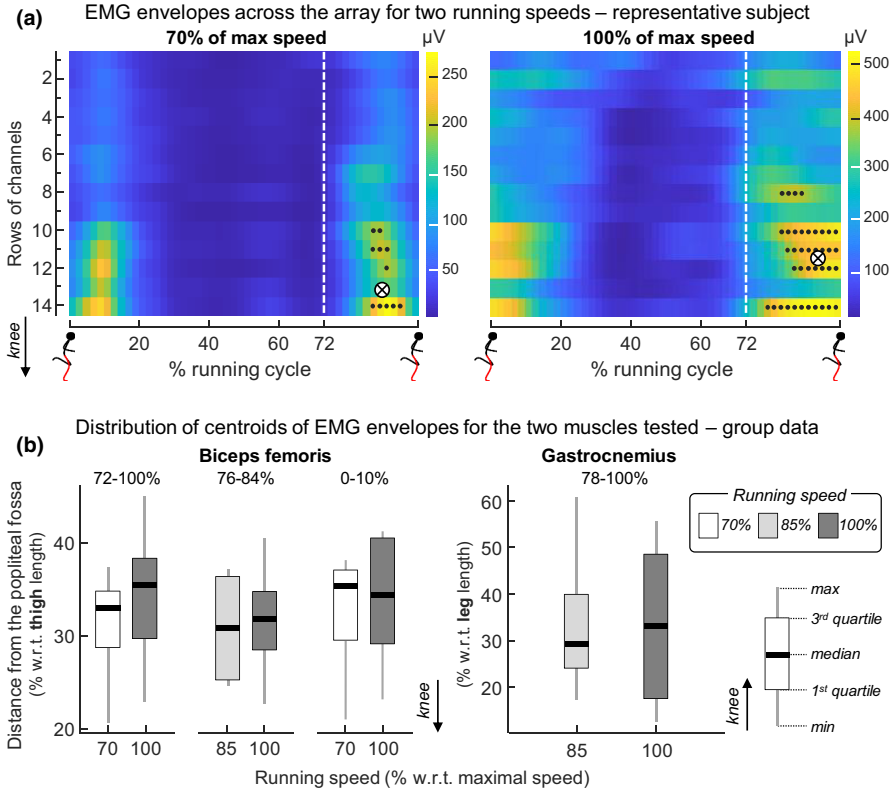

FIGURE 5 Effect of running speed on EMG distribution. (A) Spatio-temporal representation of EMG envelopes from the BF muscle, for a single participant and for the 70% (left) and 100% (right) running speeds. Small circles indicate the segmented channels whereas crossed circles denote the centroids (cf Methods[30]), both computed from 72% (vertical dashed lines) to 100% of the running cycle, when the largest, SPM{t} cluster was observed (Figure 4C). (B) Distribution of centroid values computed for the different speeds and the two muscles in correspondence of the significant, SPM{t} clusters shown in Figure 4C.

movements, power line interference, innervation zone shifts, and unbalanced impedance of the electrode-skin interface are examples of nuisance variables.[16,36,37] The former, however, is of most concern during dynamic contractions, as movement of muscles and cables is hardly suppressed. On-field detection of HD-EMG at somewhat high speeds and over long distances imposed therefore a technical challenge in our study. With the systems we developed and used for acquiring HD-EMGs[20] and biomechanical data,[28] for all subjects tested we were able to obtain high-quality signals (Figures 2 and 3). Given the electrode grid connected directly to the EMG amplifier and the reference cable was strapped around the leg, fluctuations in EMG baseline were presumably due to movement of the muscles relative to electrodes. Indeed, we observed similar, temporal variations in the baseline of monopolar EMGs and in the foot attitude in the parasagittal plane (Figure 2). The filtering of monopolar EMGs and the computation of differential EMGs successfully removed these low-frequency components, while retaining the desired, motor unit action potentials (Figure 3). It is therefore likely that the changes in EMG descriptors reported here are genuinely associated with running speed.

4.1 | Muscle excitation scales with running speed

Greater running speeds demanded greater muscle excitation, at specific periods of the running cycle though. While different studies reported the mean degree of muscle excitation to increase with running speed,[11,13–15,38,39] not all analyzed how the excitation of BF and GM changes within the running cycle. Those that did, corroborating our findings, collectively reported distinct temporal profiles of excitation between the two muscles. For instance, during submaximal speeds we observed two peaks of BF excitation—greater EMG amplitude just prior to and just after foot contact. During maximal speed, we observed a steadily high EMG amplitude, from mid swing to late stance (Figure 4A). Similar excitation profiles, at late swing and early stance, were equally reported during both treadmill and overground running, at speeds lower[17] and comparable[11,12,15] to those tested here. However, only during mid-late swing did the running speed affect the EMG amplitude. As subjects ran at greater speeds, we observed a significantly greater increase in BF excitation during late swing than during early stance (Figure 4B,C). Even though for lower running speeds, a similar temporal dependence of EMG amplitude on running speed has been reported by others.[13] Owing to the greater potential of the muscle to absorb energy when excited during eccentric contractions,[10] this pre-excitation has been suggested to offer protection against strain injuries.[13] In this context, our results would seem to extend this pre-, protective BF excitation to maximal, running speeds. Interestingly, a significant effect of running speed during late swing was similarly observed for the GM muscle—although peaks in EMG envelope were more clearly defined soon after

foot contact, significant changes with running speed were appreciated prior to foot contact (Figure 4 left column). Disconnects have arisen as per the effect of running speed on GM excitation. While two studies documented highest GM excitation from late swing to late stance,[11,15] only one reported the EMG amplitude at late swing to scale with running speed.[11] Sadly, no methodological information other than the IED used could be retrieved from both studies (38 mm in[11]; 20 mm in[15]), hindering the identification of sources of discrepancies between their results. Our results are in agreement with Kyröläinen et al.[11] In addition to imputing practical relevance to the pre-excitation of both ankle and hip extensors during sprints, our results support the importance of ensuring EMGs are mostly sensitive to muscle excitation, with a grid of electrodes or using conservatively large IEDs.[16,40]

4.2 | Regional changes in muscle excitation with running speed

Differently from previous studies, in which EMGs from discrete BF regions were compared directly,[13] we assessed regional changes in EMG amplitude from the centroid of segmented channels (Figure 5). Our decision was motivated by anatomy and sensitivity constraints. Grouping EMGs according to discrete BF regions, for example, would have to take into account inter-individual, anatomical differences. As the number of electrodes and the IED are fixed in the array, a different proportion of the muscle would be covered for subjects with different leg, and thus muscle, lengths (Figure S1). Consequently, the number of electrodes defining discrete, proximo-distal regions in both GM and BF muscles would be variable between subjects. Considering the amount of muscle shortening-lengthening during running,[9,12,39] it is further likely that different proximo-distal regions would be defined for a different set of electrodes for the same subject within the running cycle. By computing and normalizing the centroid of EMG amplitude, we likely minimized this confounder, reporting regional changes in excitation with respect to leg (GM) and thigh (BF) lengths. By neglecting the need of setting arbitrary, discretization thresholds, the centroid was expected to be sensitive to regional changes in excitation—centroids reflect the region with greatest EMGs in the array (Figure 5).

Our centroid analysis revealed to be sufficiently sensitive to detect regional changes in BF excitation with the increase in running speed. As running speed increased, we observed the BF excitation to shift proximally by 2%–10% (range) of the thigh length (Figure 5). This is in contrast with the study of Hegyi et al.[13] where no differences in EMG amplitude were reported proximo-distally in the muscle. Because of methodological differences between studies, the source of discord is not predictable. Differently from,[13] we tested subjects while running overground, near and at the maximal speed, and using a subject-specific approach to assess regional differences in EMG amplitude. While these three factors may have contributed to the spatial changes in BF excitation, running speed is the likely determinant. We observed a more proximal BF excitation only when comparing 100% and 70% of the maximal speed 75% was the maximal speed tested.[13] Our results would therefore seem to encourage the testing of extreme speeds if the site of BF injuries during running is to be studied. Yu et al.[12] suggested strain injuries may manifest at the BF-tendon junction during late stance and at the BF belly during late swing, after having observed greater BF elongation speeds during late swing. Their reasoning stems from the observation that the rate of axial strain determines the site of muscle tearing, with low and high rates resulting in tearing of the distal muscle-tendon junction and the muscle belly, respectively.[6] Similarly, in virtue of the increased ability of muscles to absorb energy before tearing when excited,[10] here we hypothesized regional changes in excitation would occur should running at speeds close to the maximum affect the site of maximal, muscle strain. Given we observed a shift in BF excitation to more proximal (central; Figure 5) regions prior to foot contact as running speed increased to the maximum, it would seem plausible to propose that this pre-excitation, as observed by others with bipolar EMGs,[11,15,39] may help protecting the muscle against tearing at BF regions located proximally from the muscle-tendon junction. Indirect verification of this hypothesis would require reproducing this study at similarly high speeds and with measurements of elongation in different BF regions, and the relevance of further exploring this possibility appears justified by the frequent, strain injuries reported for the BF muscle during sport activities demanding sprints.[1–5]

4.3 | Limitations

We see two issues potentially undermining our results and interpretations. First, we acknowledge that sample size was not identified a priori and that retention of valid running cycles was based on average rather than on instantaneous running speed. As we were unable to identify coarse figures positing the effect size of running speed on regional changes in muscle excitation in conditions similar to those tested here, we could not determine the smallest sample size associated with an acceptable (>80%) statistical power. Also, given running speed was

assessed based on average, cycle duration, we could not directly discriminate cycles during the acceleration phase (Figure 1B). These issues would open for Type II error. Conceivably, for example, one could argue that a larger sample size would have led to the emergence of significant clusters in the SPM{t} in early and mid-swing (Figure 4C). However, it should be noted that strain injuries during sprints are frequent during late swing and stance,[8,9] when we indeed observed a significant effect of speed on the degree of muscle excitation. Second, our interpretation presumes the EMG envelopes shown in Figure 4A were univocally associated with the degree of muscle excitation. This is a delicate issue, considering the highly dynamic condition we tested. Of concern here is the possibility that variations in EMG amplitude could have been associated with factors other than muscle excitation.[41] Given the in-depth pinnate architecture[16] of the two muscles assessed, we would expect the changes in muscle architecture,[42] rather than, for example, in innervation zone location,[43] to be the main, nuisance variable. To contend with this issue, we analyzed the effect of running speed on regional changes in EMG amplitude within subjects and within epochs of the running cycle, expecting muscle kinematics to remain constant across these epochs. While our assumption is seemingly plausible for the speeds we tested,[9,39] further studies are necessary to ensure the changes in EMG descriptors reported here are not due to changes in muscle kinematics.

5 | PERSPECTIVE

High-density surface EMGs revealed the location and intensity of excitation within BF change with running speed—when running speed approaches the maximum, excitation shifts proximally. This differential, spatial pattern of BF excitation, reported for the first time here, suggests low- and high-speed running impose unique demands on BF. Specific neuromuscular training may therefore be required according to the target speed, in preparation to sprints or when recovering from injuries. From a mechanisctic point of view, our results suggest the distribution of excitation within BF may serve different purposes, from protecting the muscle against failure during elongation to providing the required power in sprints. From a technical perspective, our methodology is expected to set the grounds for studying running in ecological conditions. Typically, likely due to technical constrains, overground running is studied over a limited distance (single strides[38]; 10 m[15]; 20 m[38]). The system we customized for sprint analysis[28] proved, however, to surmount these shortcomings. While our study is not the first to conduct electrophysiological and biomechanical analysis during high-speed, overground running,[12,18,19,38] it is seemingly the first to demonstrate that these studies may be extended to long-distance running in more ecological environments.

ACKNOWLEDGEMENTS

We thank Ms. Elena Di Palma for the support with data collection. Open Access Funding provided by Politecnico di Torino within the CRUI-CARE Agreement. Open Access Funding provided by Politecnico di Torino within the CRUI-CARE Agreement.

CONFLICT OF INTEREST STATEMENT

The authors declare that the research was conducted in the absence of any commercial or financial relationships that could be construed as a potential conflict of interest.

DATA AVAILABILITY STATEMENT

The data that support the findings of this study are available from the corresponding author upon reasonable request.

REFERENCES

1. Brooks JHM, Fuller CW, Kemp SPT, Reddin DB. Incidence, risk, and prevention of hamstring muscle injuries in professional Rugby union. *Am J Sports Med*. 2006;34(8):1297-1306. doi:10.1177/0363546505286022
2. Ekstrand J, Gillquist J. Soccer injuries and their mechanisms. *Med Sci Sports Exerc*. 1983;15(3):267. doi:10.1249/00005768-198315030-00014
3. Orchard J, Seward H. Epidemiology of injuries in the Australian football league, seasons 1997–2000. *Br J Sports Med*. 2002;36(1):39-44. doi:10.1136/bjsm.36.1.39
4. Edouard P, Hollander K, Navarro L, et al. Lower limb muscle injury location shift from posterior lower leg to hamstring muscles with increasing discipline-related running velocity in international athletics championships. *J Sci Med Sport*. 2021;24(7):653-659. doi:10.1016/j.jsams.2021.02.006
5. Edouard P, Navarro L, Branco P, Gremeaux V, Timpka T, Junge A. Injury frequency and characteristics (location, type, cause and severity) differed significantly among athletics ('track and field') disciplines during 14 international championships (2007–2018): implications for medical service planning. *Br J Sports Med*. 2020;54(3):159-167. doi:10.1136/bjsports-2019-100717
6. Best TM, McElhaney JH, Garrett WE, Myers BS. Axial strain measurements in skeletal muscle at various strain rates. *J Biomech Eng*. 1995;117(3):262-265. doi:10.1115/1.2794179
7. Lieber RL, Friden J. Muscle damage is not a function of muscle force but active muscle strain. *J Appl Physiol*. 1993;74(2):520-526. doi:10.1152/jappl.1993.74.2.520
8. Heiderscheit BC, Hoerth DM, Chumanov ES, Swanson SC, Thelen BJ, Thelen DG. Identifying the time of occurrence of a hamstring strain injury during treadmill running: a case study. *Clin Biomech*. 2005;20(10):1072-1078. doi:10.1016/j.clinbiomech.2005.07.005

9. Thelen DG, Chumanov ES, Hoerth DM, et al. Hamstring muscle kinematics during treadmill sprinting. *Med Sci Sports Exerc*. 2005;37(1):108-114. doi:10.1249/01.MSS.0000150078.79120.C8
10. Garrett WE, Safran MR, Seaber A v, Glisson RR, Ribbeck BM. Biomechanical comparison of stimulated and nonstimulated skeletal muscle pulled to failure. *Am J Sports Med*. 1987;15(5):448-454. doi:10.1177/036354658701500504
11. Kyröläinen H, Komi PV, Belli A. Changes in muscle activity patterns and kinetics with increasing running speed. *J Strength Cond Res*. 1999;13(4):400-406. doi:10.1519/1533-4287(1999)013<0400:CIMAPA>2.0.CO;2
12. Yu B, Queen RM, Abbey AN, Liu Y, Moorman CT, Garrett WE. Hamstring muscle kinematics and activation during overground sprinting. *J Biomech*. 2008;41(15):3121-3126. doi:10.1016/j.jbiomech.2008.09.005
13. Hegyi A, Gonçalves BAM, Finni T, Cronin NJ. Individual region-and muscle-specific hamstring activity at different running speeds. *Med Sci Sports Exerc*. 2019;51(11):2274-2285. doi:10.1177/036354658701500504
14. Higashihara A, Ono T, Kubota J, Okuwaki T, Fukubayashi T. Functional differences in the activity of the hamstring muscles with increasing running speed. *J Sports Sci*. 2010;28(10):1085-1092. doi:10.1080/02640414.2010.494308
15. Kuitunen S, Komi PV, Kyröläinen H. Knee and ankle joint stiffness in sprint running. *Med Sci Sports Exerc*. 2002;34(1):166-173. doi:10.1097/00005768-200201000-00025
16. Vieira TM, Botter A. The accurate assessment of muscle excitation requires the detection of multiple surface electromyograms. *Exerc Sport Sci Rev*. 2021;49(1):23-34. doi:10.1249/JES.0000000000000240
17. Wang L, Hong Y, Xian LJ. Muscular activity of lower extremity muscles running on treadmill compared with different Overground surfaces. *Am J Sports Med*. 2014;2(4):161-165. doi:10.12691/ajssm-2-4-8
18. Wank V, Frick U, Schmidtbleicher D. Kinematics and electromyography of lower limb muscles in overground and treadmill running. *Int J Sports Med*. 1998;19(7):455-461. doi:10.1055/s-2007-971944
19. Frishberg BA. An analysis of overground and treadmill sprinting. *Med Sci Sports Exerc*. 1983;15(6):478-485. doi:10.1249/00005768-198315060-00007
20. Cerone GL, Botter A, Gazzoni M. A modular, smart, and wearable system for high density sEMG detection. *IEEE Trans Biomed Eng*. 2019;66(12):3371-3380. doi:10.1109/TBME.2019.2904398
21. Salis F, Bertuletti S, Scott K, et al. A wearable multi-sensor system for real world gait analysis. *Annu Int Conf IEEE Eng Med Biol Soc*. 2021;2021:7020-7023. doi:10.1109/EMBC46164.2021.9630392
22. Tokutake G, Kuramochi R, Murata Y, Enoki S, Koto Y, Shimizu T. The risk factors of hamstring strain injury induced by high-speed running. *J Sports Sci Med*. 2018;17(4):650-655.
23. Spiriev B. *IAAF Scoring Tables of Athletics*. 2017. Accessed December 15, 2021 https://www.iaaf.org/download/download?filename=b031e933-c722-4d0d-bfb9-9399ff8fb26f.pdf&urlslug=IAAF%20Scoring%20Tables%20of%20Athletics%20-%20Outdoor%20
24. Agre JC. Hamstring injuries. *Sports Med*. 1985;2(1):21-33. doi:10.2165/00007256-198502010-00003
25. dos Anjos F v, Gazzoni M, Vieira TM. Does the activity of ankle plantar flexors differ between limbs while healthy, young subjects stand at ease? *J Biomech*. 2018;81:140-144. doi:10.1016/j.jbiomech.2018.09.018
26. Hermens HJ, Freriks B, Disselhorst-Klug C, Rau G. Development of recommendations for SEMG sensors and sensor placement procedures. *J Electromyogr Kinesiol*. 2000;10(5):361-374. doi:10.1016/s1050-6411(00)00027-4
27. Cerone GL, Giangrande A, Ghislieri M, Gazzoni M, Piitulainen H, Botter A. Design and validation of a wireless body sensor network for integrated EEG and HD-sEMG acquisitions. *IEEE Trans Neural Syst Rehabil Eng*. 2022;30:61-71. doi:10.1109/TNSRE.2022.3140220
28. Salis F, Bertuletti S, Bonci T, della Croce U, Mazzà C, Cereatti A. A method for gait events detection based on low spatial resolution pressure insoles data. *J Biomech*. 2021;127:110687. doi:10.1016/j.jbiomech.2021.110687
29. Watanabe K, Kouzaki M, Moritani T. Regional neuromuscular regulation within human rectus femoris muscle during gait. *J Biomech*. 2014;47(14):3502-3508. doi:10.1016/j.jbiomech.2014.09.001
30. Vieira TM, Merletti R, Mesin L. Automatic segmentation of surface EMG images: improving the estimation of neuromuscular activity. *J Biomech*. 2010;43(11):2149-2158. doi:10.1016/j.jbiomech.2010.03.049
31. Friston KJ, Holmes AP, Worsley KJ, Poline JP, Frith CD, Frackowiak RSJ. Statistical parametric maps in functional imaging: a general linear approach. *Hum Brain Mapp*. 1994;2(4):189-210. doi:10.1002/hbm.460020402
32. Pataky TC, Vanrenterghem J, Robinson MA. The probability of false positives in zero-dimensional analyses of one-dimensional kinematic, force and EMG trajectories. *J Biomech*. 2016;49(9):1468-1476. doi:10.1016/j.jbiomech.2016.03.032
33. Penny W, Henson R. Analysis of variance. In: Friston K, Ashburner J, Kiebel S, Nichols T, Penny W, eds. *Statistical Parametric Mapping*. Elsevier; 2007:166-177. doi:10.1016/B978-012372560-8/50013-9
34. Pataky TC. Generalized n-dimensional biomechanical field analysis using statistical parametric mapping. *J Biomech*. 2010;43(10):1976-1982. doi:10.1016/j.jbiomech.2010.03.008
35. Pataky TC, Vanrenterghem J, Robinson MA. Zero- vs. one-dimensional, parametric vs. non-parametric, and confidence interval vs. hypothesis testing procedures in one-dimensional biomechanical trajectory analysis. *J Biomech*. 2015;48(7):1277-1285. doi:10.1016/j.jbiomech.2015.02.051
36. Merletti R, Aventaggiato M, Botter A, Holobar A, Marateb H, Vieira TM. Advances in surface EMG: recent progress in detection and processing techniques. *Crit Rev Biomed Eng*. 2010;38(4):305-345. doi:10.1615/CritRevBiomedEng.v38.i4.10
37. Vigotsky AD, Halperin I, Trajano GS, Vieira TM. Longing for a longitudinal proxy: acutely measured surface EMG amplitude is not a validated predictor of muscle hypertrophy. *Sports Med*. 2022;52(2):193-199. doi:10.1007/s40279-021-01619-2
38. Higashihara A, Nagano Y, Ono T, Fukubayashi T. Differences in activation properties of the hamstring muscles during overground sprinting. *Gait Posture*. 2015;42(3):360-364. doi:10.1016/j.gaitpost.2015.07.002
39. Schache AG, Dorn TW, Wrigley TV, NAT B, Pandy MG. Stretch and activation of the human biarticular hamstrings across a range of running speeds. *Eur J Appl Physiol*. 2013;113(11):2813-2828. doi:10.1007/s00421-013-2713-9

40. Vieira TMTM, Botter A, Muceli S, Farina D. Specificity of surface EMG recordings for gastrocnemius during upright standing. *Sci Rep*. 2017;7(1):1-11. doi:10.1038/s41598-017-13369-1
41. Vigotsky AD, Halperin I, Lehman GJ, Trajano GS, Vieira TM. Interpreting signal amplitudes in surface electromyography studies in sport and rehabilitation sciences. *Front Physiol*. 2018;8:1-15. doi:10.3389/fphys.2017.00985
42. Vieira TM, Bisi MC, Stagni R, Botter A. Changes in tibialis anterior architecture affect the amplitude of surface electromyograms. *J Neuroeng Rehabil*. 2017;14(1):81. doi:10.1186/s12984-017-0291-5
43. Mancebo FD, Cabral H v, de Souza LML, de Oliveira LF, Vieira TM. Innervation zone locations distribute medially within the pectoralis major muscle during bench press exercise. *J Electromyogr Kinesiol*. 2019;46:8-13. doi:10.1016/j.jelekin.2019.03.002

SUPPORTING INFORMATION

Additional supporting information can be found online in the Supporting Information section at the end of this article.

How to cite this article: Cerone GL, Nicola R, Caruso M, Rossanigo R, Cereatti A, Vieira TM. Running speed changes the distribution of excitation within the biceps femoris muscle in 80 m sprints. *Scand J Med Sci Sports*. 2023;00:1-12. doi:10.1111/sms.14341